

● *Original Contribution*

## IMAGING OF GAPS IN DIGITAL JOINTS BY MEASUREMENT OF ULTRASOUND TRANSMISSION USING A LINEAR ARRAY

HIDEYUKI HASEGAWA,<sup>#,\*</sup> MICHIKO MATSUURA,<sup>†</sup> HIROSHI SATO,<sup>†</sup> TERUKO YAMAMOTO<sup>†</sup>  
and HIROSHI KANAI<sup>\*,#</sup>

<sup>#</sup>Graduate School of Biomedical Engineering; <sup>\*</sup>Graduate School of Engineering; and <sup>†</sup>Graduate School of Dentistry,  
Tohoku University, Sendai, Japan

(Received 14 December 2007; revised 18 August 2008; in final form 15 September 2008)

**Abstract**—In orthodontic dentistry for young subjects, it is important to assess the degree of growth of the jaw bones to determine the optimum time for treatment. The structure of the digital joint changes with age, with such changes correlating to the degree of bone growth (including jaw bones). There are two gaps in the digital joint of a young subject, one of which disappears with aging. In the present study, a method for noninvasive assessment of such change in the structure of a digital joint was examined, in which continuous-wave ultrasound is radiated to a digital joint by a single-element ultrasonic transducer. This continuous ultrasound, which passes through the digital joint, is received by a linear array ultrasonic probe situated opposite the transducer. The probe simultaneously realizes pulse–echo imaging and imaging of transmission ultrasound, which passes through the joint. Using this experimental apparatus, the existence and position of a gap can be detected clearly by imaging the transmission ultrasound on a pulse–echo image. In basic experiments, continuous-wave ultrasound generated by a planar or focused transducer was radiated to a gap between two acrylic bars, which simulated that in a digital joint; transmission ultrasound, which passed through the gap, was measured with a linear array probe. The basic experimental results showed that a gap with a width >0.4 mm is detectable and that the width at half maximum of the amplitude profile of the received transmission ultrasound that passed through the gap correlated with the width of the gap. Furthermore, in the preliminary *in vivo* experiments, transmission ultrasound that passed through two gaps in the case of a child was clearly imaged by the proposed method, and that which passed through only one gap in the case of an adult was also imaged. These results show the possibility for the use of the proposed method to noninvasively assess the change in the structure of a joint as a result of aging. (E-mail: [hasegawa@ecei.tohoku.ac.jp](mailto:hasegawa@ecei.tohoku.ac.jp)) © 2009 World Federation for Ultrasound in Medicine & Biology.

**Key Words:** Bone age, Digital joint, Continuous-wave ultrasound, Ultrasound transmission, Linear array.

### INTRODUCTION

In orthodontic dentistry for young subjects, it is important to assess the degree of growth of the jaw bones to determine the optimum time for treatment. The ossification of bones in a hand is often used for assessment of bone age, such ossification being evaluated by x-ray imaging of a hand and wrist (Tanner et al. 1975; Rucci et al. 1995; Wit et al. 2005; Jones and Ma 2005). In addition, Khal et al. (2008) have recently proposed a method by which the degree of bone growth is assessed based on the maturation of the cervical spine. The bone maturity assessed by this method was found to correlate well with

that assessed by hand radiography. This method would be useful because the cervical spine is always seen on the lateral cephalometric radiograph. Although these methods give an accurate estimate of bone age, exposure of healthy subjects to x-rays is inevitable.

Because ultrasound is useful for noninvasive diagnosis of bone, many studies on ultrasonic measurement of bone have been conducted. Wells (1975) reported the speed of sound and ultrasonic absorption in bone, whereas Williams (1991) predicted the propagation of slow and fast waves propagating through bone by Biot's theory (Biot 1962) and also experimentally measured these waves. Otani and colleagues extensively investigated slow and fast waves (Hosokawa and Otani 1997, 1998; Hosokawa et al. 1997; Otani 2005), which propagate in bone marrow and the contained hard structure, respectively. Therefore, the amplitude of a slow-wave

Address correspondence to: Hideyuki Hasegawa, Department of Biomedical Engineering, Graduate School of Biomedical Engineering, Tohoku University, 6-6-05 Aramaki-aza-Aoba, Aoba-ku, Sendai 980-8579, Japan. E-mail: [hasegawa@ecei.tohoku.ac.jp](mailto:hasegawa@ecei.tohoku.ac.jp)

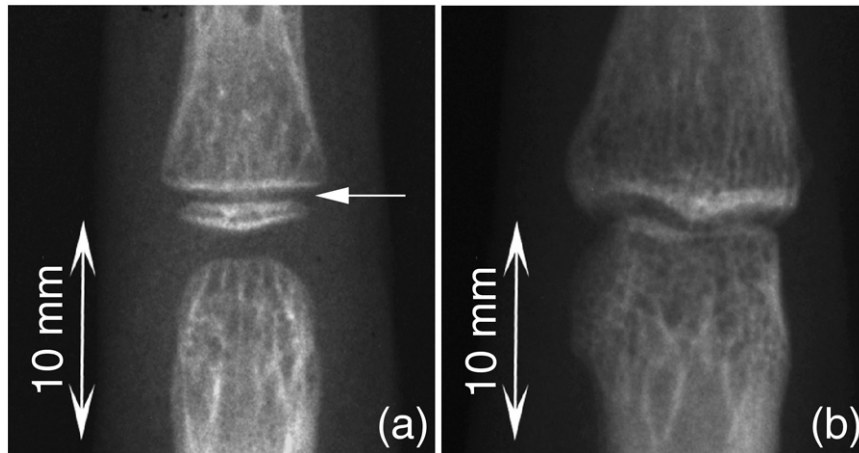


Fig. 1. X-ray image of the second joint of the middle finger. (a) 5-year-old male. The arrowhead indicates the gap that disappears with aging. (b) 26-year-old female.

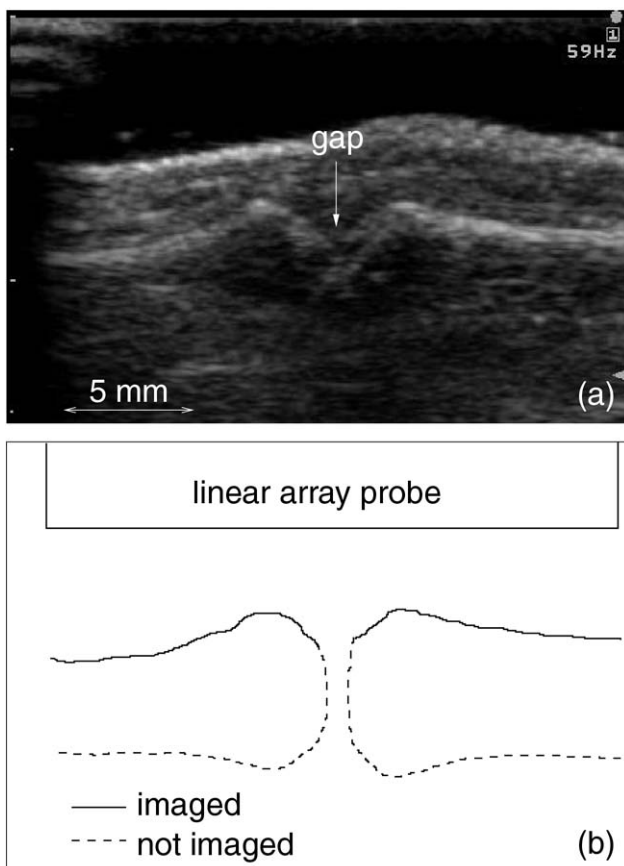


Fig. 2. (a) Ultrasonic B-mode image of the second joint of the middle finger of a 33-year-old male. (b) Illustration of regions imaged by pulse-echo imaging.

propagating through the cancellous or trabecular bone increases as the hard structure decreases, whereas that of a fast wave decreases. The hard structure in trabecular bone decreases because of osteoporosis and, thus, a method has recently been developed to quantitatively estimate bone density and quality by measuring the amplitude change of these waves that cannot be obtained only from the attenuation coefficient of bone (Otani 2005). Speed-of-sound and attenuation of ultrasound in bone is used widely for characterization of bone (Asai *et al.* 1996; Wear 2000, 2001a; Bossy *et al.* 2004). However, the structure of bone is complex, and the measured sound velocity shows a significant dispersion. Many studies have been conducted to identify the sources of this dispersion (Droin *et al.* 1998; Wear 2000, 2001b), and Häät *et al.* (2006) have attempted to generalize the measurement of sound velocity in bone. Furthermore, methods for estimating attenuation and spacing of cancellous bone structures by analyzing backscattered ultrasound have been developed (Wear 2003; Pereira *et al.* 2004) because the aforementioned methods require measurement of transmission ultrasound through the bone, and it is difficult to apply such methods to bone deep inside the body. All of these methods measure speed-of-sound and attenuation of ultrasound propagating through, or backscattered from, a large bone to estimate the bone density for diagnosis of osteoporosis in elderly subjects, the quality of bone being the main focus.

The present study was focused on the structure of a joint. As shown by a method using x-ray imaging (Tanner *et al.* 1975; Rucci *et al.* 1995; Wit *et al.* 2005; Jones and Ma 2005), the structure of a joint of a young subject changes because of aging. In the case of a digital joint of a young subject, there are two gaps, one of which disappears with aging. The present study investigated an

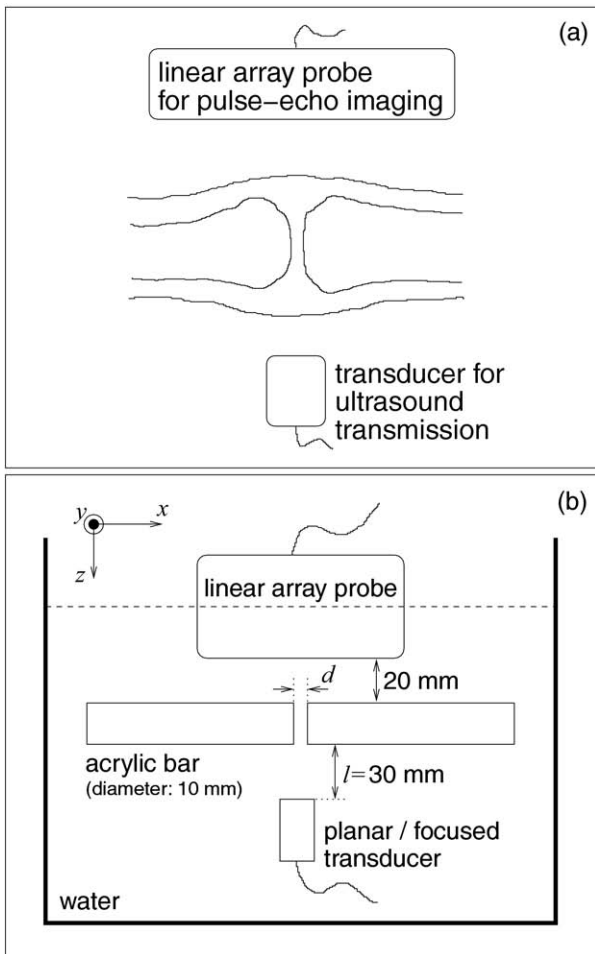


Fig. 3. (a) Measurement apparatus to realize pulse-echo imaging and ultrasound transmission imaging simultaneously. (b) Schematic diagram of experimental setup. Both planar and focused transducers were used for ultrasound transmission.

ultrasonic-based method to noninvasively assess such change in the structure of a digital joint by using ultrasound transmission through a joint. Weigel et al. (1982) conducted ultrasound transmission imaging using sacrificed dogs seven to eight weeks of age. They used collimated ultrasound (plane wave) for transmission, the transmitted ultrasound being focused by an acoustic lens system. Their system achieved a spatial resolution of approximately 1 mm at an ultrasonic frequency of 2 MHz. In the present study, higher-frequency ultrasound was used for ultrasound transmission through a digital joint, the gap of such joint usually being <1 mm. Furthermore, focused and unfocused ultrasound were used because the latter may be better for transmission through a narrow gap. Ultrasound transmitted through a gap was measured by a linear array ultrasonic probe. This experimental setup enables simultaneous pulse-echo imaging and ultrasound transmission imaging. The feasibility of this method was investigated by basic experiments using acrylic bars. Furthermore, initial *in vivo* imaging was conducted for child and adult subjects.

Current methods for assessment of the bone maturity using x-rays are accurate and exposure to radiation is relatively low. However, ultrasonic methods would supplement x-ray methods because of their absolute noninvasiveness and potential for use in a wide range of medical institutions, because the cost of ultrasonic equipment is lower than that of x-ray equipment. Unfortunately, no equipment for imaging ultrasound transmission is now commercially available, and thus a new experimental system was used in this study to examine the basic concepts of the proposed method.

**MATERIALS AND METHODS**

*Growth of bone in digital joints*

Figure 1a and b show x-ray images of the second joints of middle fingers of a 5-year-old male and 26-year-

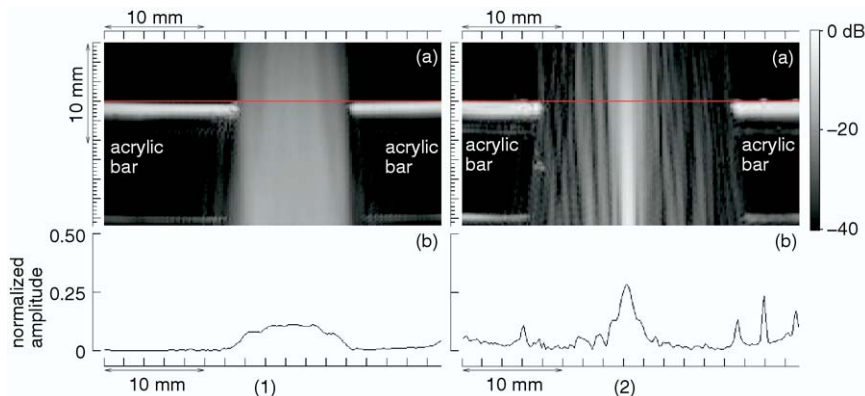


Fig. 4. (a) Imaged pattern and (b) amplitude profile along the red line in (a) of transmission ultrasound: (1) planar, 5 MHz; (2) focused, 7 MHz.

old female, respectively. The gap indicated by the white arrow in Fig. 1a disappears because of aging. Therefore, a joint with developing bone can be differentiated from that with mature bone by identifying whether there are two gaps. In addition, the width of the gap indicated by the white arrow in Fig. 1a can be used for evaluation of bone age. This study was approved by the Ethics Committee on Clinical Investigation, Graduate School of Dentistry, Tohoku University, and was performed in accordance with the policy of the Declaration of Helsinki; all subjects gave informed consent.

*Conceptual overview*

Ultrasonic B-mode imaging is useful for morphologic diagnosis of organs. Figure 2a shows a B-mode

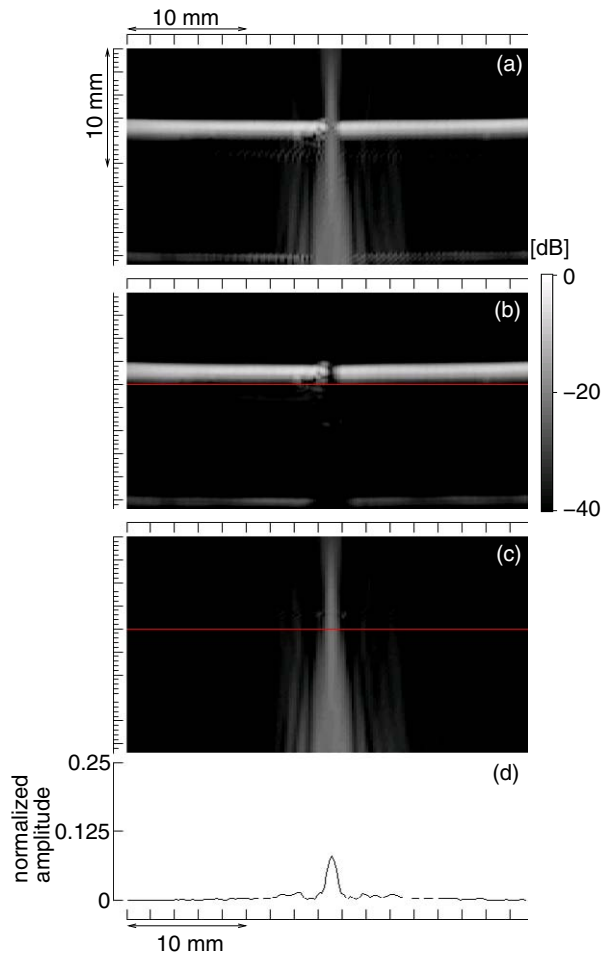


Fig. 5. Example of analysis in basic experiments (diameters of bars: 10 mm; width of gap: 0.6 mm; planar transducer for ultrasound transmission): B-mode images (a) with and (b) without exposure of transmission ultrasound, respectively. The transmitting transducer was placed on the bottom and the linear array probe was placed at the top. (c) Subtraction image obtained from (a) and (b). (d) Amplitude profile along the red line in (c).

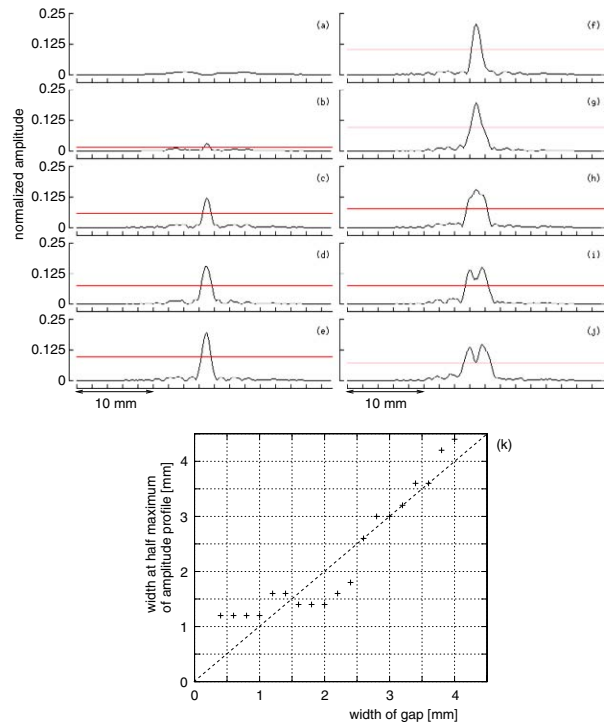


Fig. 6. Amplitude profiles at different widths of the gap (planar transducer, diameter of bars: 10 mm): (a) 0 mm, (b) 0.4 mm, (c) 0.8 mm, (d) 1.2 mm, (e) 1.6 mm, (f) 2 mm, (g) 2.4 mm, (h) 2.8 mm, (i) 3.2 mm and (j) 3.6 mm. (k) Width at half maximum of the amplitude profile plotted as a function of the gap width (diameter of bars: 10 mm). Planar transducer was used, and widths at half maximum were obtained from 10 image frames at each gap width  $d$ .

image of the second joint of the middle finger of a 33-year-old male. A gap in the joint can be recognized in the B-mode image shown in Fig. 2a. However, the tissue structure in the joint is poorly imaged because the incident ultrasound is almost perfectly reflected by the near surfaces of bones and the pulse-echo imaging can only assess the shape of the near surfaces (illustrated by the solid curves in Fig. 2b). In addition, the exact position of a gap is somewhat unclear because the image pattern in a gap is inhomogeneous, as shown in Fig. 2a, similar to that of the surrounding soft tissue. The reason is that the acoustic impedance of cartilage (of course, there is soft tissue in a joint) is much closer to that of soft tissue compared with that of bone (Töyräs *et al.* 2003), and there is no distinct echo from a gap.

To overcome this drawback, in this study transmission of continuous ultrasound through a gap in a joint was imaged in combination with pulse-echo imaging to clearly assess the existence of gaps and their positions. A linear array ultrasonic probe was positioned, as shown in Fig. 3a, for pulse-echo imaging of a gap. A single-element ultrasonic transducer opposite the linear array



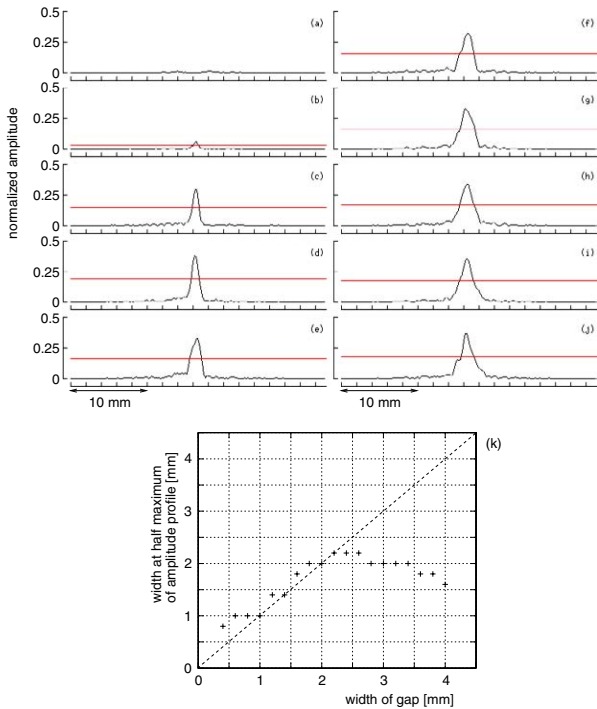


Fig. 7. Amplitude profiles at different widths of the gap (focused transducer, diameter of bars: 10 mm): (a) 0 mm, (b) 0.4 mm, (c) 0.8 mm, (d) 1.2 mm, (e) 1.6 mm, (f) 2 mm, (g) 2.4 mm, (h) 2.8 mm, (i) 3.2 mm and (j) 3.6 mm. (k) Width at half maximum of the amplitude profile plotted as a function of the gap width (diameter of bars: 10 mm). Focused transducer was used, and widths at half maximum were obtained from 10 image frames at each gap width  $d$ .

was used for irradiation of continuous-wave ultrasound for transmission through the gap. Transmission ultrasound that passed through the gap was received by the linear array. Ultrasound for transmission was irradiated continuously, and transmission ultrasound that passed through the gap was imaged together with the pulse-echo image. Imaged transmission ultrasound clearly showed the existence of a gap, and the transmission pattern provided information on the width of the gap.

*Experimental setup*

As shown in Fig. 3b, two acrylic bars were placed between a 10-MHz linear array probe (UST-5545, Aloka Co., Ltd., Tokyo, Japan) for imaging and a transducer for generation of continuous-wave ultrasound to penetrate a gap with width  $d$  between the two acrylic bars. The gap simulated that between bones in a joint. Transmission ultrasound that passed through the gap was measured by the linear array probe. Planar (5Z10I-C, Tokimec Co., Ltd., Tokyo, Japan) and focused (7Z10I-PF30-C-K445, Tokimec Co., Ltd.) transducers, driven by 5-MHz and 7-MHz continuous signals, respectively, were used for

generation of transmission ultrasound. The distance between the surface of the transducer and the lower edges of the acrylic bars was set at 30 mm, which corresponds to the focal distance of the focused transducer. The distance between the surface of the linear array probe and the upper edges of the acrylic bars was set at 20 mm, which corresponds to the elevational focal distance (fixed focus using acoustic lens). Using this apparatus, the ultrasound transmitted through the gap could be imaged together with the object (acrylic bars). RF signals, which contain both continuous-wave and pulsed ultrasound produced by the transducer and array probe, respectively, and are received by the array probe, were sampled at 40 MHz.

As described previously, it is essential for evaluation of bone age of a young subject to investigate whether one or two gaps exist between the bones in a joint. Furthermore, it is desirable that the width of the gap be assessed from the measured pattern of transmission ultrasound. In basic experiments, transmission ultrasound was measured by changing the gap width  $d$  from 0–4 mm, with increments of 0.2 mm to investigate how a small gap can be detected and whether the width

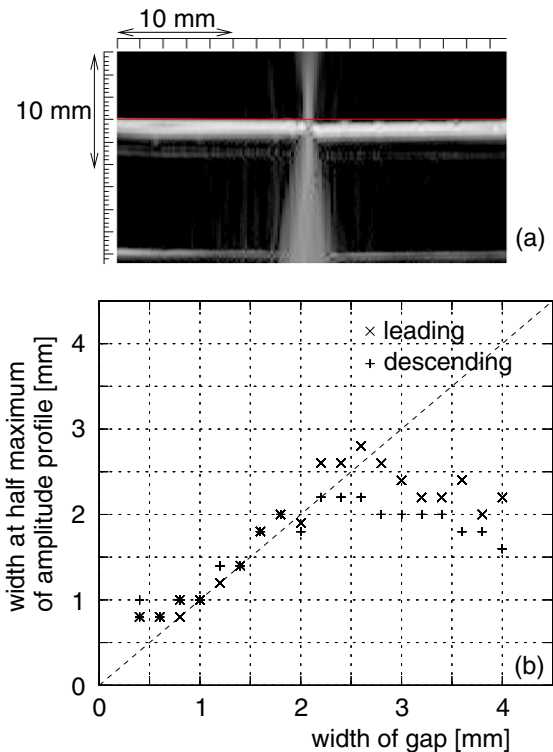


Fig. 8. (a) Example of measurement of an amplitude profile at the leading edge (indicated by red line) of the echo from the upper surface of the bar (diameter of bars: 10 mm). (b) Widths at half maxima of amplitude profiles obtained at the leading and descending edges of the echo from the upper surface of the bar.

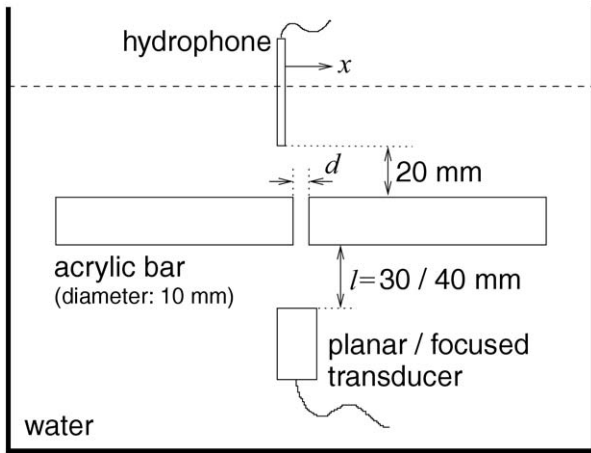


Fig. 9. Illustration of measurement of sound field emitted from a gap.

of such a gap can be evaluated using the measured transmission ultrasound.

*Difference between imaged patterns of transmission ultrasound produced by planar and focused transducers*

Figure 4(1-a) and (2-a) show the imaged transmission ultrasound produced by the planar and focused

Table 1. Widths at half maxima  $\Delta w$  of the amplitude profiles of transmission ultrasound measured for different distances between the focused transducer for transmitting ultrasound and the lower surface of the acrylic bar (10 mm in diameter)

Width of gap $d$ (mm)	Distance between focused transducer and lower surface of bar (mm)	Width at half maximum $\Delta w$ (mm)
0.6	30	0.8
0.6	40	0.7
2.0	30	1.8
2.0	40	1.8

transducers for transmission, respectively. In these figures, gap width  $d$  was set at about 5 mm and 9 mm, respectively, *i.e.*,  $>4$  mm (maximum gap width in basic experiments), to visualize the imaged pattern of transmission ultrasound in a wider area. Figure 4(1-b) and (2-b) show the profiles of the amplitudes of ultrasound signals received by the linear array probe along the red lines in Fig. 4(1-a) and (2-a). The imaged radiation pattern of the focused transducer (Fig. 4[2-a]) was rather complex compared with that of the planar transducer (Fig. 4[1-a]), the latter being suitable for imaging a wider gap. However, as the measured transmission ultrasound produced by the focused transducer showed a high in-

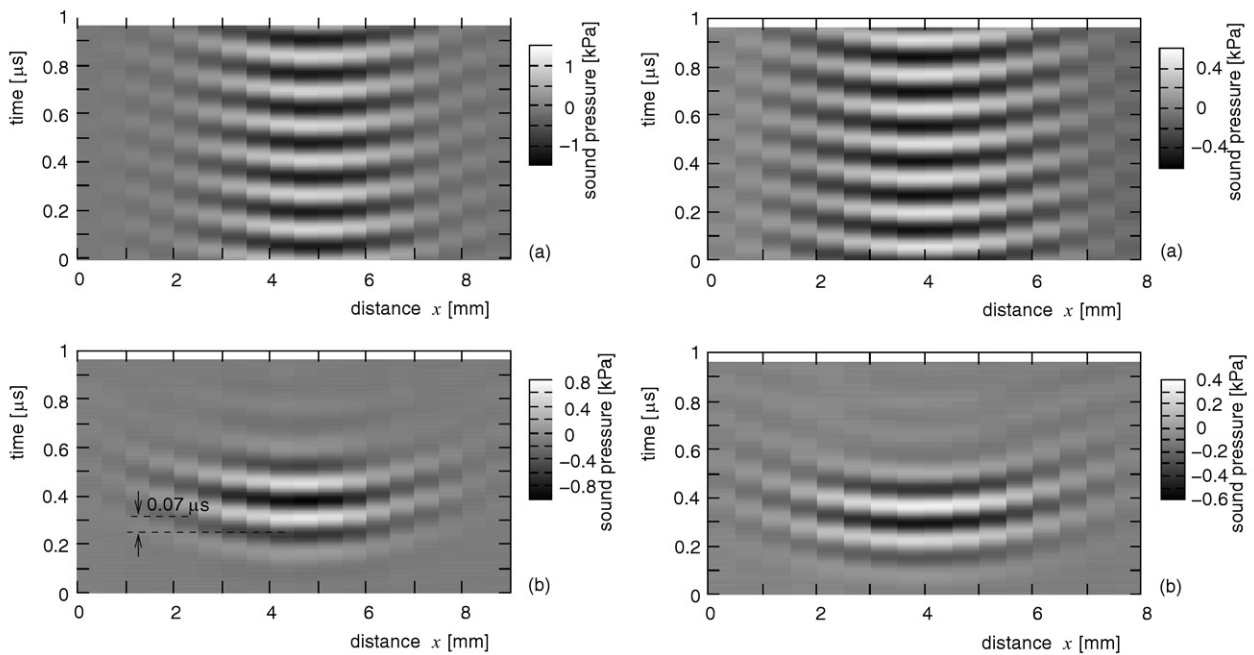


Fig. 10. Sound fields measured by a hydrophone when a focused transducer for ultrasound transmission was placed (1) 30 mm and (2) 40 mm away from the lower surface of the bar (diameter of bars: 10 mm). (a) Continuous and (b) pulsed ultrasound were emitted from a focused transducer.

tensity within a narrow area (width at half maximum: 2 mm), it would be useful for penetration of cartilage and tissue in a joint because the attenuation in such tissue is much greater than that in water. Thus, the focused transducer was used in the following preliminary *in vivo* imaging, whereas both the planar and focused transducers were used in the basic experiments.

## BASIC EXPERIMENTAL RESULTS

### Measurements with the planar transducer

Figure 5a and b show B-mode images with and without exposure of transmission ultrasound produced by the 5-MHz planar transducer. The width of the gap in Fig. 5 was 0.6 mm. Ultrasound transmitted through the gap was clearly imaged. In the basic experiments, the object was stationary. Therefore, as shown in Fig. 5c, only transmission ultrasound that passed through the gap could be imaged by subtracting the RF signals without exposure from those with exposure, which were received

by the linear array probe. Figure 5d shows the profile of the echo amplitude along the red line shown in Fig. 5c.

Using the same procedure, the amplitude profiles at the same depth, shown by the red line in Fig. 5c, were obtained for other widths  $d$  of gaps. Figure 6a–j show the amplitude profiles at various gap widths  $d$  from 0–3.6 mm. The amplitude profile was obtained at the descending edge of the echo from the upper surface of the bars, as indicated by the red lines in Fig. 5. As can be seen in Fig. 6b, transmission ultrasound was detected at a gap width  $d$  larger than 0.4 mm. In Fig. 6a–j, the red lines show the width at half maximum  $\Delta w$  of each amplitude profile. Figure 6k shows the width at half maximum  $\Delta w$  plotted as a function of gap width  $d$ . In Fig. 6k, widths at half maximum  $\Delta w$  obtained from 10 image frames are plotted at each gap width  $d$ . As shown in Fig. 6k, there is a correlation between the width  $\Delta w$  of the amplitude profile and the gap width (correlation coefficient between the actual and measured gap widths: 0.93 [overall], 0.60

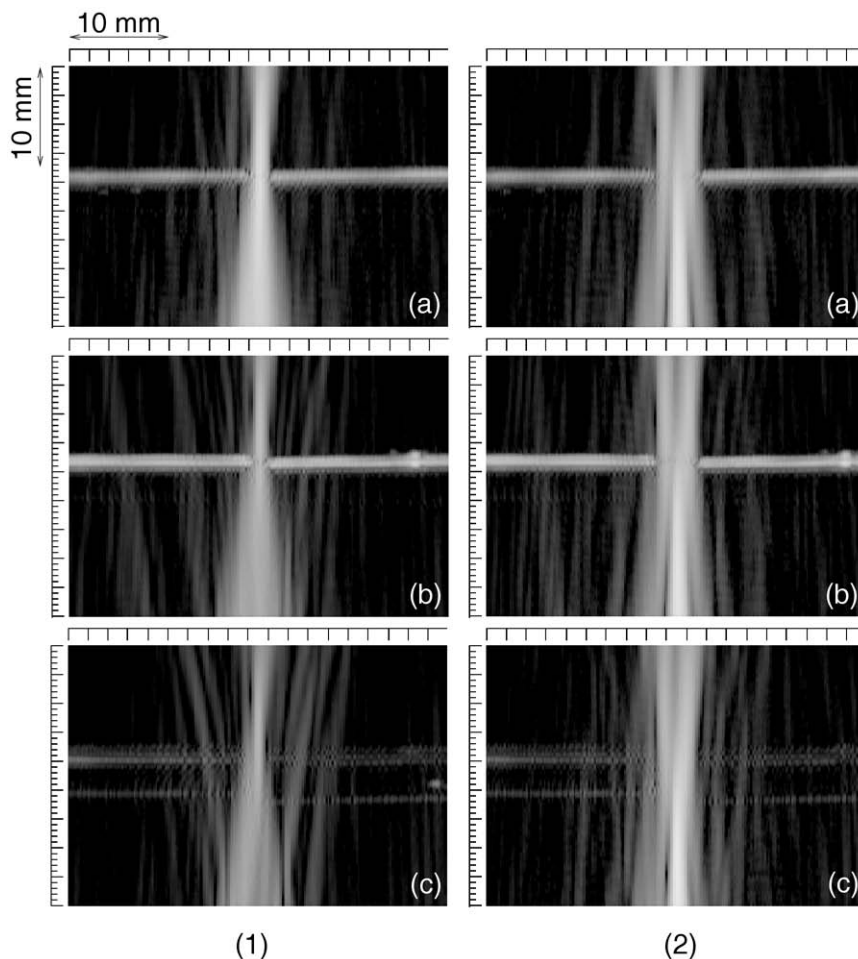


Fig. 11. Imaged transmission ultrasound in B-mode images (diameter of acrylic bars: 10 mm). Gap widths  $d$  were set at (1) 0.6 mm and (2) 2.0 mm. The elevational positions  $y$  of the bars were set at (a) 0 mm, (b) 2.5 mm and (c) 5 mm.

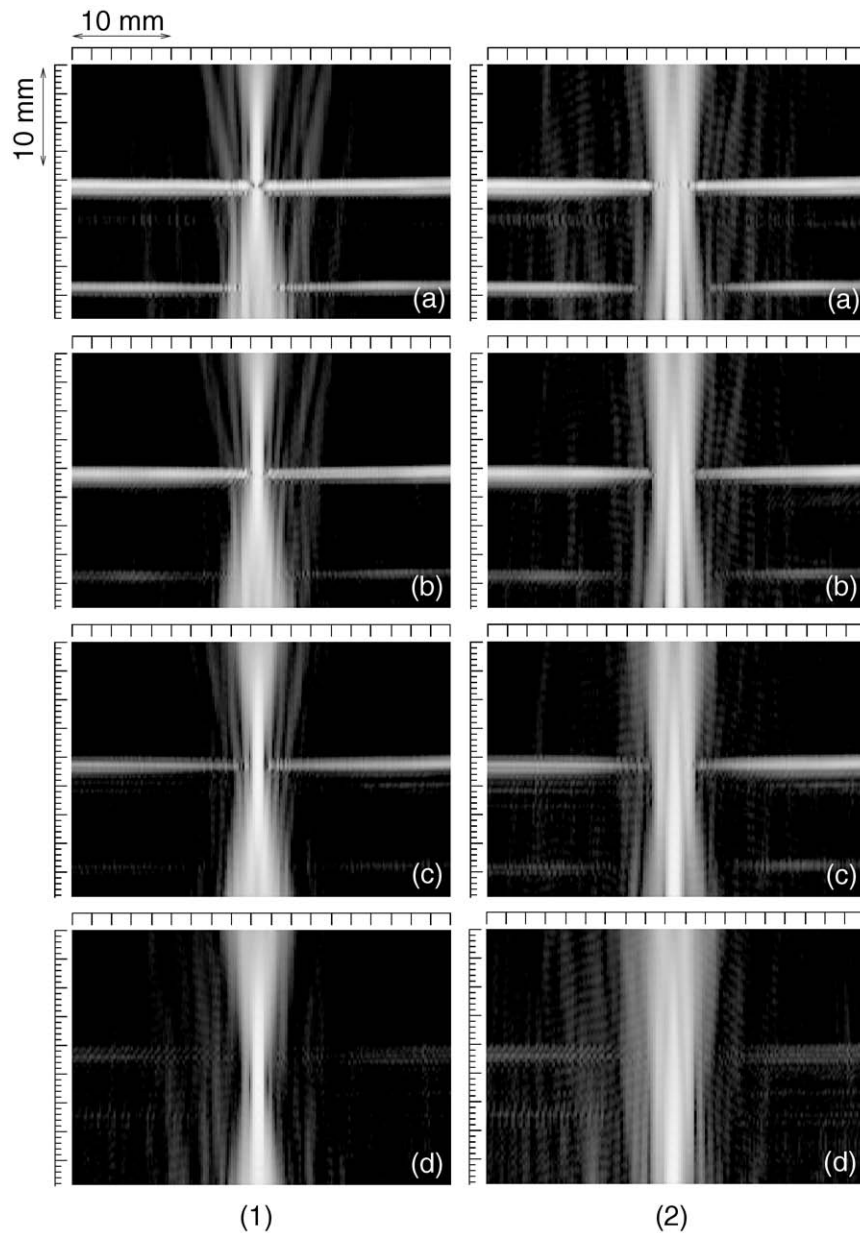


Fig. 12. Imaged transmission ultrasound in B-mode images (diameter of acrylic bars: 6 mm). Gap widths  $d$  were set at (1) 0.6 mm and (2) 2.0 mm. The elevational positions  $y$  of the bars were set at (a) 0 mm, (b) 1 mm, (c) 2 mm and (d) 3 mm.

$[d = 0.4$  to  $2$  mm],  $0.98$  [ $d = 2$  to  $4$  mm]). These results show the possibility of using the proposed method to measure gap width  $d$ . However, the correlation is weak in the range of gap width  $d < 2$  mm in the case of the planar transducer.

#### *Measurements with the focused transducer*

Figure 7a–j show the amplitude profiles measured with the focused transducer. As in the case of the planar transducer, ultrasound transmitted through the gap can be

detected at a gap width  $d > 0.4$  mm. However, the amplitude profile does not change so much in the range of gap width  $d > 2$  mm because the width at half maximum of the amplitude profile of the original radiation pattern of the focused transducer was 2 mm, as shown in Fig. 4(2-b). However, the amplitude of the received transmission ultrasound was two times larger than that of the planar transducer, which is a great advantage for penetrating the cartilage and tissue in a joint. Figure 7k shows the width at half maximum  $\Delta w$  of an amplitude



Table 2. Widths at half maxima  $\Delta w$  of the amplitude profiles of transmission ultrasound measured for different elevational positions  $y$  of the bars (10 mm in diameter)

Gap width $d$ (mm)	Elevational position $y$ (mm)	Width at half maximum $\Delta w$ (mm)
0.6	0	0.8
0.6	2.5	0.9
0.6	5	1.0
2.0	0	1.8
2.0	2.5	1.8
2.0	5	1.6

profile plotted as a function of gap width  $d$ . In Fig. 7k, widths at half maximum  $\Delta w$  obtained from 10 image frames are plotted at each gap width  $d$ . There is no correlation between the width at half maximum  $\Delta w$  and gap width  $d$  in the range of gap width  $>2$  mm, which corresponds to the fact that the amplitude profile does not change in that range, as shown in Fig. 7a–j. However, there is a strong correlation at a gap width  $d < 2$  mm (correlation coefficient between the actual and measured gap widths: 0.7 [overall], 0.94 [ $d = 0.4$  to 2 mm] and  $-0.94$  [ $d = 2$  to 4 mm]). Therefore, a focused transducer is useful, especially for imaging a narrow gap in a digital joint. As shown in Fig. 1, the typical width of a gap in a digital joint is  $<2$  mm. Therefore, the focused transducer was used in the subsequent experiments.

Widths at half maxima shown in Fig. 7k were measured at depth positions assigned by referring to the descending edge of the echo from the upper surface of the acrylic bar. Figure 8 shows the widths at half maxima measured at the leading edge of the echo from the upper surface; the measured widths  $\Delta w$  in Fig. 8 are similar to those in Fig. 7k. In this study, widths at half maxima  $\Delta w$  were measured at the descending edge in the subsequent experiments because stable measurements of  $\Delta w$  can be achieved as long as measurement is done at the leading or descending edge of the echo from the upper surface of the bars.

The sound pressure distribution measured with a hydrophone, which scans the sound field in the horizontal direction  $x$  (the longitudinal axis of the bar), as shown in Fig. 9, was shown in Figure 10(1-a). Gap width  $d$  was set to be 0.6 mm, and the distance between the lower surface of the bar and the transmitting transducer was set at 30 mm. To more clearly observe how the ultrasound wave propagated, pulsed ultrasound was irradiated from the transmitting transducer as shown in Fig. 10(1-b), which shows that a spherical wave was emitted from the gap. The distance between the hydrophone and the source of the spherical wave, which was estimated from the time delay ( $p = 0.07 \mu\text{s}$ , as shown in Fig. 10[1-b]) between signals received at two different horizontal po-

sitions  $x$ , was 19 mm. Therefore, the source was estimated to be located at the gap on the level of the upper surface of the bar. In the diagnostic ultrasound equipment used, dynamic focusing was applied to the signals received by the array elements. In this case, the width of the ultrasound beam becomes the narrowest at the position of the source of the spherical wave.

Figure 10(2) shows the sound field measured when the distance  $l$  between the lower surface of the bar and the transmitting transducer was set at 40 mm, and Table 1 shows a comparison of the widths at half maxima  $\Delta w$  measured at  $l = 30$  and 40 mm. The wave pattern was similar to that in Fig. 10(1), and the width at half maximum  $\Delta w$  measured at  $l = 40$  mm was similar to that at  $l = 30$  mm. However, the amplitude of transmission ultrasound that passed through the gap decreased 50%, as shown in Fig. 10(2). It is considered that more energy can enter a gap when the beam width is narrower at the entrance of a gap. These results indicate that it is better to locate the focal point of a transmitting transducer at the lower surface of the bar.

#### Measurements of gaps between bars with different diameters

Acrylic bars 10 mm and 6 mm in diameter were used to create gaps, as shown in Fig. 3b. Transmission ultrasound that passed through gaps with different widths  $d$  of 0.6 and 2.0 mm were measured for the different positions,  $y$ , of the acrylic bars in the elevational direction to investigate the influence of the alignment of the bars.

Figures 11 and 12 show the B-mode images and Tables 2 and 3 show the widths at half maxima  $\Delta w$  of the amplitude profiles of transmission ultrasound measured at each setting of gap width  $d$  and elevational position  $y$ . As shown in Tables 2 and 3, the measured width at half maximum  $\Delta w$  does not change when the elevational position  $y$  is less than half the radius of the bar, and the difference between widths at half maxima of the ampli-

Table 3. Widths at half maxima  $\Delta w$  of the amplitude profiles of transmission ultrasound measured for different elevational positions  $y$  of the bars (6 mm in diameter)

Gap width $d$ (mm)	Elevational position $y$ (mm)	Width at half maximum $\Delta w$ (mm)
0.6	0	0.7
0.6	1	0.7
0.6	2	0.6
0.6	3	0.7
2.0	0	1.7
2.0	1	1.7
2.0	2	1.4
2.0	3	1.9

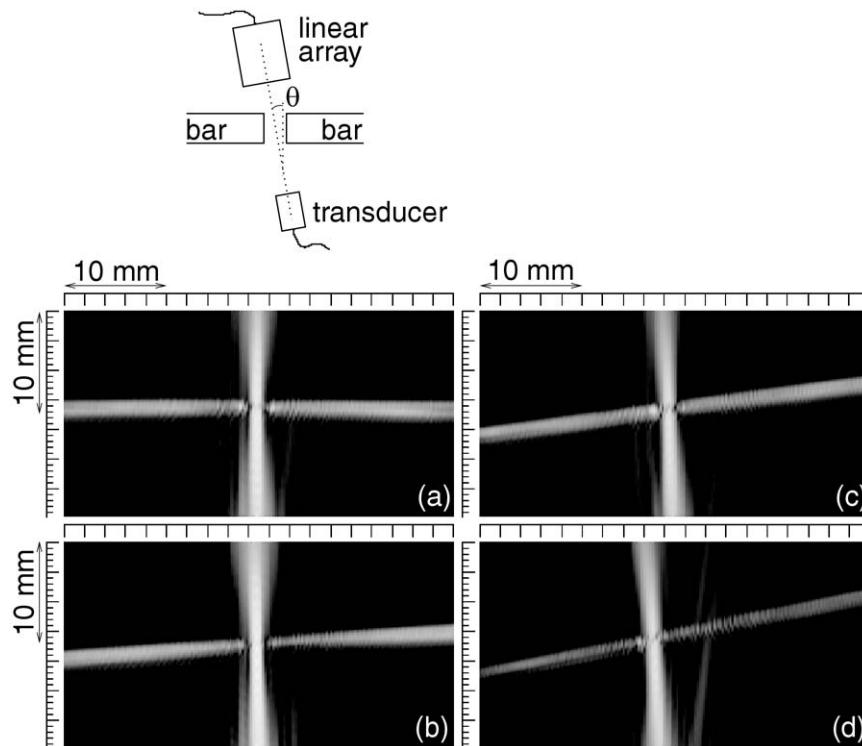


Fig. 13. Imaged transmission ultrasound through the gap (width  $d$ : 0.6 mm) at different angles of incident  $\theta$  of (a) 0 degree, (b) 2.5 degrees, (c) 5 degrees and (d) 7.5 degrees. Diameter of bars was 10 mm.

tude profiles obtained for 6-mm and 10-mm acrylic bars was 0.1 mm when  $y = 0$ .

#### Measurements at different angles of incidence between ultrasound and the gap

The amplitude profile of transmission ultrasound would be influenced by the angle of incidence between the ultrasound beam radiated by the focused transducer and the gap. In the previous section, the widths at half maxima measured for the acrylic bars with different diameters were similar when the elevational position  $y$  was zero. Therefore, the influence of the angle of incidence was investigated using acrylic bars 10 mm in diameter by setting the elevational position  $y$  at zero. The gap width  $d$  was set at 0.6 mm. Figure 13 shows images of transmission ultrasound through the gap at different angles of incidence  $\theta = 0, 2.5, 5$  and  $7.5$  degrees. Table 4 shows the width at half maximum  $\Delta w$  measured at these angles of incidence  $\theta$ . As shown in Fig. 13, although the change in the alignment was obvious, even when the angle of incidence was 2.5 degrees, the measured widths at half maxima were similar, as shown in Table 4.

#### Preliminary in vivo imaging

Figure 14(1-a) and (2-a) show x-ray images of the hands of a 5-year-old male and a 26-year-old female,

respectively, and Fig. 14(1-b) and (2-b) are enlarged views of the second joints of their middle fingers. One of the two gaps found in the child subject indicated by the white arrow in Fig. 14(1-b) is not found in the joint of the 26-year-old female shown in Fig. 14(2-b).

Figure 14(1-c) shows an ultrasound B-mode image with exposure of transmission ultrasound (focused, 7 MHz) for the 5-year-old male, and Fig. 14(2-c) shows that of the 26-year-old female. The widths of gaps of these two subjects are from 1–2 mm, and the focused transducer was used with consideration of the results of the basic experiments. In Fig. 14(1-c), transmission ultrasound that passed through the two regions in the joint can be clearly recognized in the case of the 5-year-old male. On the other hand, in the B-mode image of the 26-year-old female (Fig. 14[2-c]), applied focused ultrasound passed through only one region. These results

Table 4. Widths at half maxima  $\Delta w$  of the amplitude profiles of transmission ultrasound measured at different angles of incidence  $\theta$  (diameter of bars: 10 mm)

Angle of incidence $\theta$ (deg.)	Width at half maximum $\Delta w$ (mm)
0	0.7
2.5	0.7
5	0.7
7.5	0.8

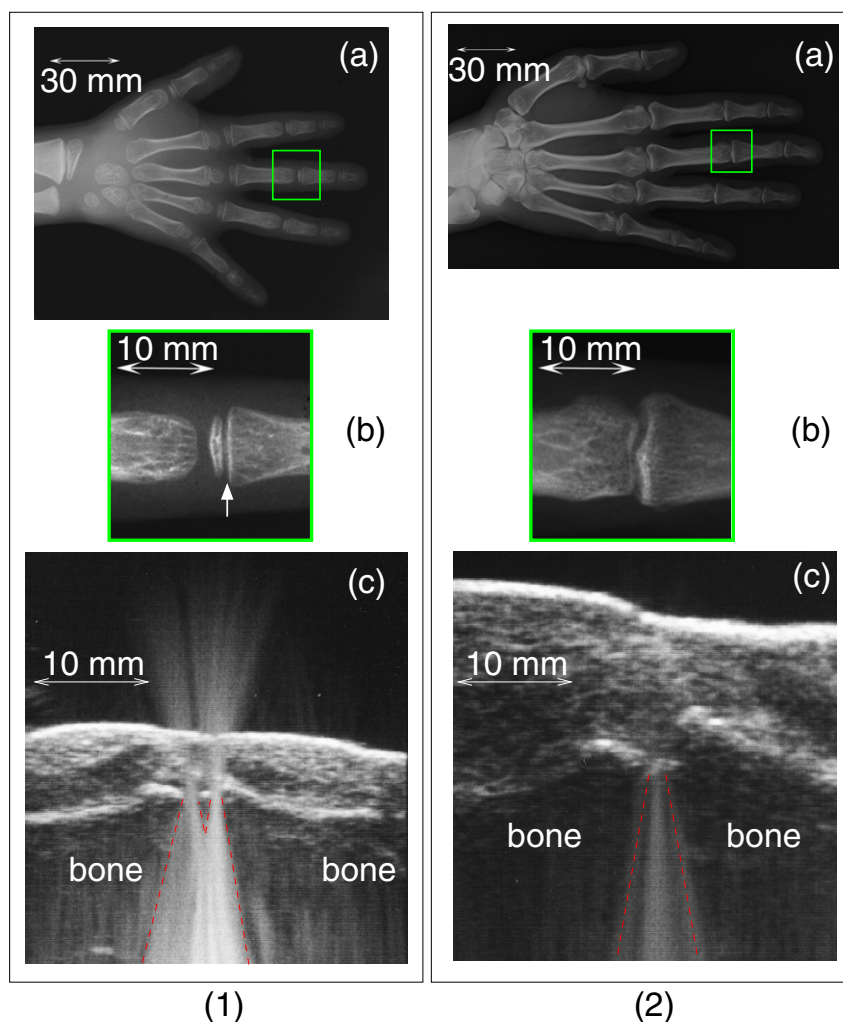


Fig. 14. *In vivo* imaging of transmission ultrasound through the second joint of the middle finger. (1) 5-year-old male. (2) 26-year-old female. (a) X-ray image. (b) Enlarged x-ray image of the second joint. (c) Ultrasound B-mode image of the second joint, with exposure of transmission ultrasound (focused, 7 MHz).

correspond well to the structures of the joints shown by x-ray images and indicate that the proposed method has potential for noninvasive assessment of the change in structure of a joint because of aging.

## DISCUSSION

As shown in Fig. 4, depending on the type of a transducer (planar or focused), transmission ultrasound received by a linear array probe showed different patterns in the B-mode image. The lateral variation in the amplitude of transmission ultrasound depends on the type of transducer (planar or focused). However, variation in the direction of depth should not occur because continuous-wave ultrasound was used to penetrate a gap in cases of both the planar and focused transducers. However, there are variations in

the direction of depth, especially in the case of the focused transducer. Such a variation in the direction of depth is considered to depend on the receiving focus of the linear array probe. Although dynamic focusing was applied to the received signals in the used diagnostic equipment, the relationship between the receiving focus setting and the imaged pattern of transmission ultrasound should be further investigated in the future to reduce the spatial inhomogeneity in the original imaged radiation pattern shown in Fig. 4.

It was found that a focused transducer should be used for transmitting ultrasound through a gap with a width  $< 2$  mm, which corresponds to the typical width of a gap in a digital joint. Through basic experiments using acrylic bars, it was found that the width at half maximum  $\Delta w$  of the amplitude profile of transmission ultrasound

correlated well with actual gap width  $d$  under the following conditions:

- (1) The focal point of a transmitting transducer is located at the lower surface of the bar.
- (2) The elevational positions  $y$  of the bars are set to be less than half of the radius of the bar.
- (3) The width at half maxima  $\Delta w$  is measured at the leading or descending edge of the echo from the upper surface of the bar.

To realize stable *in vivo* measurements, in future work it will be important to develop a measurement system in which the above conditions are maintained.

To apply this method to other larger joints, the separation between a transducer for ultrasound transmission and an imaging probe needs to be increased. To keep the focal position of a transducer as it was in the present study, a different transducer and different probe must be used to increase the separation. The frequency of ultrasound may need to be changed because of the increase of the distance between the skin surface and a joint. In addition, the type of transducer (planar or focused) may need to be considered to image a wider gap in a larger joint. Therefore, the optimum frequency of transmission ultrasound and the type of transducers (planar or focused) should be more thoroughly investigated because the frequency of ultrasound significantly influences the spatial resolution. In this preliminary study, different frequencies were used for the planar and focused transducers. A set consisting of planar and focused transducers operated at the same frequency would be required to investigate the difference between these transducers, and sets of transducers at different frequencies would be required to investigate the optimum frequency.

Although there are many things to be investigated further as described here, the proposed method would enable the tomographic imaging of a digital joint. The combination of pulse–echo imaging and tomographic imaging should be useful for diagnosis of joint structures.

## CONCLUSION

The structure of a digital joint changes with aging. There are two gaps in a digital joint of a young subject, one that disappears with aging. To noninvasively assess such change in a digital joint, in this study continuous-wave ultrasound was radiated through a gap between two acrylic bars, which simulated the gap in the digital joint. Transmission ultrasound was measured with a linear array probe for imaging. The basic experimental results showed that a gap with a width  $>0.4$  mm can be imaged. In the case of a planar transducer, the width at half maximum of the amplitude profile of received transmission ultrasound that passed through the gap correlated with the width of the gap when the gap was  $>2.0$  mm.

On the other hand, the width at half maximum obtained using a focused transducer correlated with the gap width when the gap was  $<2.0$  mm. From these results, a focused transducer is considered to be preferable for the measurement of a gap in a digital joint whose width is typically  $<2$  mm. Furthermore, in the preliminary *in vivo* experiments, transmission ultrasound that passed through two gaps was clearly imaged by the proposed method in the case of a child subject, whereas transmission ultrasound that passed through only one gap was imaged in the case of an adult subject. These results show the possibility of using the proposed method to noninvasively assess the change in the structure of a joint because of aging.

## REFERENCES

- Asai H, Kanai H, Chubachi N. Noninvasive method for measuring velocity of leaky surface skimming compressional wave propagating on bone surface. *Electron Lett* 1996;32:2290–2291.
- Biot MA. Generalized theory of acoustic propagation in porous dissipative media. *J Acoust Soc Am* 1962;34:1254–1264.
- Bossy E, Talmant M, Defontaine M, Patat F, Laugier P. Bidirectional axial transmission can improve accuracy and precision of ultrasonic velocity measurement in cortical bone: A validation on test materials. *IEEE Trans Ultrason Ferroelectr Freq Control* 2004;51:71–79.
- Droin P, Berger G, Laugier P. Velocity dispersion of acoustic waves in cancellous bone. *IEEE Trans Ultrason Ferroelectr Freq Control* 1998;45:581–592.
- Häät G, Padilla F, Cleveland RO, Laugier P. Effects of frequency-dependent attenuation and velocity dispersion on *in vitro* ultrasound velocity measurements in intact human femur specimens. *IEEE Trans Ultrason Ferroelectr Freq Contr* 2006;53:39–51.
- Hosokawa A, Otani T. Ultrasonic wave propagation in bovine cancellous bone. *J Acoust Soc Am* 1997;101:558–562.
- Hosokawa A, Otani T, Suzaki T, Kubo Y, Takai S. Influences of trabecular structure on ultrasonic wave propagation in bovine cancellous bone. *Jpn J Appl Phys* 1997;36:3233–3237.
- Hosokawa A, Otani T. Acoustic anisotropy in bovine cancellous bone. *J Acoust Soc Am* 1998;103:2718–2722.
- Jones G, Ma D. Skeletal age deviation assessed by the Tanner-Whitehouse 2 method is associated with bone mass and fracture risk in children. *Bone* 2005;36:352–357.
- Khal HAA, Wong WK, Rabie ABM. Elimination of the hand-wrist radiographs for maturity assessment in children needing orthodontic therapy. *Skeletal Radiol* 2008;37:195–200.
- Otani T. Quantitative estimation of bone density and bone quality using acoustic parameters of cancellous bone for fast and slow waves. *Jpn J Appl Phys* 2005;44:4578–4582.
- Pereira WCA, Bridal SL, Coron A, Laugier P. Singular spectrum analysis applied to backscattered ultrasound signals from *in vitro* human cancellous bone specimens. *IEEE Trans Ultrason Ferroelectr Freq Control* 2004;51:302–312.
- Rucci R, Coppini G, Nicoletti I, Cheli D, Valli G. Automatic analysis of hand radiographs for the assessment of skeletal age: A subsymbolic approach. *Comput Biomed Res* 1995;28:239–256.
- Tanner J, Whitehouse R. *Assessment of Skeletal Maturity and Prediction of Adult Height (TW2 method)*. New York: Academic Press, 1975.
- Töyräs J, Laasanen MS, Saarakkala S, Lammi MJ, Rieppo J, Kurkuärvi J, Lappalainen R, Jurvelin JS. Speed of sound in normal and degenerated bovine articular cartilage. *Ultrasound Med Biol* 2003;29:447–454.
- Wear KA. The effects of frequency-dependent attenuation and dispersion on sound speed measurements: Applications in human trabec-

- ular bone. *IEEE Trans Ultrason Ferroelectr Freq Control* 2000; 47:265–273.
- Wear KA. Ultrasonic attenuation in human calcaneus from 0.2 to 1.7 MHz. *IEEE Trans Ultrason Ferroelectr Freq Control* 2001a;48:602–608.
- Wear KA. A stratified model to predict dispersion in trabecular bone. *IEEE Trans Ultrason Ferroelectr Freq Control* 2001b;48:1079–1083.
- Wear KA. Characterization of trabecular bone using the backscattered spectral centroid shift. *IEEE Trans Ultrason Ferroelectr Freq Control* 2003;50:402–407.
- Weigel JP, Cartee RE, Marich KW. Preliminary study on the use of ultrasonic transmission imaging to evaluate the hip joint in the immature dog. *Ultrasound Med Biol* 1983;9:371–378.
- Wells PNT. Absorption and dispersion of ultrasound in biological tissue. *Ultrasound Med Biol* 1975;1:369–376.
- Williams JL. Ultrasonic wave propagation in cancellous and cortical bone: Prediction of some experimental results by Biot's theory. *J Acoust Soc Am* 1992;91:1106–1112.
- Wit JM, Rekers-Mombarg LT, Cutler GB, Crowe B, Beck TJ, Roberts K, Gill A, Chaussain JL, Frisch H, Yturriaga R, Attanasio AF. Growth hormone (GH) treatment to final height in children with idiopathic short stature: Evidence for a dose effect. *J Pediatr* 2005; 146:45–53.